ACADEMIC PRESS

Available online at www.sciencedirect.com
SCIENCE DIRECT®

Journal of Colloid and Interface Science 259 (2003) 331–337

JOURNAL OF Colloid and Interface Science

www.elsevier.com/locate/jcis

Comparison of the structural properties of isomorphously substituted Fe in mordenite zeolites prepared by different methods

Mohamed M. Mohamed,[a,*] N.S. Gomaa,[b] M. El-Moselhy,[c] and N.A. Eissa [b]

[a] *Chemistry Department, Faculty of Science, Benha University, Benha, Egypt*
[b] *Mössbauer Laboratory, Physics Department, Faculty of Science, Al-Azhar University, Cairo, Egypt*
[c] *Chemistry Department, Faculty of Science, Al-Azhar University, Cairo, Egypt*

Received 28 June 2002; accepted 19 December 2002

Abstract

Fe was introduced in mordenite zeolite by means of ion exchange either in solid or in liquid state. The iron loading (50–200 wt%), iron precursor ($FeSO_4{\cdot}7H_2O$ and $FeCl_3$), and mordenite starting material (NH_4M, HM, and NaM) were varied during the exchange processes. The Fe species were characterized by N_2 adsorption measurements as well as by XRD and Mössbauer spectroscopies. The Fe–mordenite samples prepared by liquid-state ion exchange attained remarkable Fe dispersion and surface areas higher than those of the parent. It was found that Fe^{3+} ions, which substituted the framework Al and accordingly occupied tetrahedral sites, were decreased with Fe loadings with concomitant increase in Fe^{3+}-occupied octahedral sites. The latter sites disappeared at 20 K to provoke the superparamagnetic α-Fe_2O_3 in different particles size. The acid leaching (0.1 M HCl, 333 K, 3 h) of the samples showed the disappearance of the most highly distorted extra-framework Fe^{3+} species, providing an indication of their presence on the external surface. On the other hand, a hematite phase was detected in the solid-state ion exchange of $FeCl_3$ with either HM or NH_4M at the loading of 100% Fe. More correlations between Mössbauer data on one hand and XRD and texturing properties on the other hand were evaluated and discussed.

Keywords: Iron–mordenites; Ion exchange; Acid leaching; XRD; Texturing; Mössbauer spectroscopy

1. Introduction

Selective catalytic reduction (SCR) of NO_x to N_2 has attracted much interest at the academic level looking for an effective catalyst that practically can be utilized. This is due to the fast growing of NO_x, which arises as a component of the exhausts of automobiles and of the emissions of various chemical processes. The impact of NO_x on the atmosphere involves its sharing in the destruction of the ozone layer in the stratosphere. Sincere efforts have been paid to efficiently convert NO_x into N_2, or to the direct decomposition of NO to N_2 and O_2, to protect our global environment.

So far, two main catalysts were employed for SCR of NO_x to N_2. The first catalyst was Cu–ZSM-5, which showed high activity under dry reaction conditions. Whereas, in a wet environment, which is inevitably produced in the combustion process within the engine, the catalyst undergoes poisoning followed by dealumination and physical breakdown [1,2]. The second catalyst was Fe–ZSM-5, which showed activity toward NO_x removal greater than that of Cu–ZSM-5, especially in the presence of reducing agents [3]. In addition, the former catalyst showed greater resistance to poisoning by water vapor and further exhibited greater durability [4,5].

Identification of Fe species, their locations, and coordination are prerequisites to understanding their high activities in zeolites following calcination temperatures. The presence of low coordinated Fe^{2+} or Fe^{3+} cations in zeolite makes them much more susceptible to adsorb NO than those of highly coordinated ones [6,7]. This can be obtained by using the ion exchange process for preventing the formation of highly coordinated Fe^{3+} species, which were capable of forming aggregated oxide clusters. The latter clusters were found to be inactive for either the decomposition of nitrogen oxides or the SCR of NO [8–10]. Unfortunately, it has been reported that the majority of Fe^{3+} ions incorporated in pentasil zeolites (especially, ZSM-5 and mordenite) showed relatively

* Corresponding author.
E-mail address: mohmok2000@yahoo.com (M.M. Mohamed).

0021-9797/03/$ – see front matter
doi:10.1016/S0021-9797(02)00221-7

good coordination inside zeolites and thus inaccessibility to smaller molecules such as NO can be obtained.

By way of understanding more about the chemistry of Fe in zeolites, which is principally affected by preparation conditions, this study was undertaken to examine the coordination and morphology of Fe ions after incorporation into mordenite zeolites. Recently, a poorly coordinated Cu^{2+} in mordenite was obtained for the purpose of enhancing the adsorption of NO. The excellent reactivity and accessibility shown by Cu^{2+} in mordenite to NO evoked us to obtain benefit of the unusual stability and durability of Fe in zeolite compared with the corresponding Cu one [4,5]. Two different preparation routes, namely, liquid-state and solid-state ion exchange, were employed. In the present work Fe–mordenite samples were studied by XRD, Mössbauer spectroscopy, and N_2 adsorption to characterize the oxidation states and environment of Fe species in mordenite as well as their morphologies, texture, and pore structure.

2. Experimental

2.1. Sample preparation

H–mordenite [$Na_8(AlO_2)_8(SiO_2)_{40}\cdot 24H_2O$] supplied by Conteka (IDN, 122-90-003) was transformed into the sodium form (NaM; Si/Al = 5.0) by ion exchange with NaOH (0.1 M) at 298 K under permanent stirring. This step was repeated three times prior to filtering off the ion exchange products, which were then washed by distilled water and finally dried at 393 K for 12 h.

Two different routes were used for the preparation of Fe–mordenite samples. First, NaM was ion exchanged with varying solutions of $FeSO_4\cdot 7H_2O$ (Merck) at 323 K. The exchange process was carried out in a refluxing flask under nitrogen while stirring. The pH was maintained in the range $6 < pH < 7$ during the exchange. An exhaustive exchange so as to prepare different loadings of Fe was obtained, giving samples formally represented by, within nominal molarities indicated between brackets, 50% FeM (3.6×10^{-3} M), 100% FeM (7.1×10^{-3} M), 150% FeM (11.0×10^{-3} M), and 200% FeM (14.0×10^{-3} M), was obtained. The latter samples have the following Fe contents (uptake percentages): 49.8, 98.4, 148.7, and 198.9%, respectively. These values prove that all of the supplied Fe remains in the samples. This may lead us to presume that there is no precipitation of a small amount of FeOOH in the pore system [5]. The overexchange at 150 and 200% was achieved on the basis of $[FeOH]^+$ formation that replaces one Na^+ and, thus, $1Fe^{2+} = 2Na^+$; i.e., an overexchange of up to 200% could be produced [11]. After 24 h, the ion exchange products were filtered, washed, and dried under vacuum at 353 K. Finally, the catalysts were calcined for 12 h at 823 K under a stream of nitrogen gas. The percentages of exchanged Fe in Na–mordenite were determined spectrophotometrically [12] by UV (Jasco V-570 unit) absorption of thiocyanate–Fe complex in the presence of CTAB at 308 nm; the procedure is sensitive to Fe concentrations as low as 0.6 ppm Fe.

The second method was a solid-state ion exchange process in which $FeCl_3$, at 100% loading, was mixed with either NH_4M [$(NH_4)_8(AlO_2)_8(SiO_2)_{40}\cdot 24H_2O$], supplied from Conteka (CBR 30A; IDN, 123-90-003), or HM. These samples were denoted as 100% Fe–NH_4M and 100% Fe–HM, respectively, on the basis of $1Fe^{3+} = 3Na^+$. The latter percentages only suggest the amount of Fe present on zeolite samples but do not necessarily represent a complete ion exchange process. The mixing process was carried out in a grinder under ambient pressure for 2 h. This solid-state ion exchange process was initiated by heating at 473 K (5 K/min) under vacuum conditions for 1 day. Finally, the samples were calcined at 823 K in N_2 atmosphere for 5 h in order to activate the Fe–mordenite samples. More details about the sample preparation can be found elsewhere [13].

2.2. Sample characterization

X-ray diffraction patterns of calcined samples were taken using a Philips diffractometer of type PW 1390 using CuKα at room temperature. Measurements of the samples were carried out in the 2θ range of 5–60°, under the conditions of 30 kV and 10 mA, at a scanning rate of $2\theta = 2°$.

Specific surface areas and average pore diameters of various samples were obtained by the BET method at the liquid N_2 temperature (77 K) using a conventional volumetric apparatus. The samples were outgassed at 573 K for 3 h before starting the run. A highly pure (99%) N_2 was used as adsorbate.

The Mössbauer spectra (MS) were recorded at room temperature and at 20 K, using a constant acceleration spectrometer. The source activity was 3.70 GBq of ^{57}Co in a Cr matrix. Iron metal was used as a reference for the isomer shift (IS). Sample cooling to temperatures as low as 20 K was achieved using an industrial instrument cryogenic CTI system. A Neocera LTC-11 temperature controller was used.

3. Results and discussion

3.1. Liquid-state ion exchange

The MS of Fe–mordenite samples, with different Fe loadings, measured at room temperature are shown in Fig. 1. All spectra were fitted into three overlapping paramagnetic doublets. Analysis of the Mössbauer parameters (Table 1) of these doublets revealed the presence of two doublets due to Fe^{3+} in different distorted octahedral symmetry [$Fe^{3+}(O)_1$ and $Fe^{3+}(O)_2$] along with another doublet due to Fe^{3+} occupying tetrahedral sites, $Fe^{3+}(T)$. The presence of Fe^{3+} in tetrahedral sites provided evidence for its location in framework T sites substituting for Al. On the other hand, the Fe^{3+} in octahedral sites corresponds to the extra-framework Fe^{3+} that either occludes inside zeolite channels or presents on

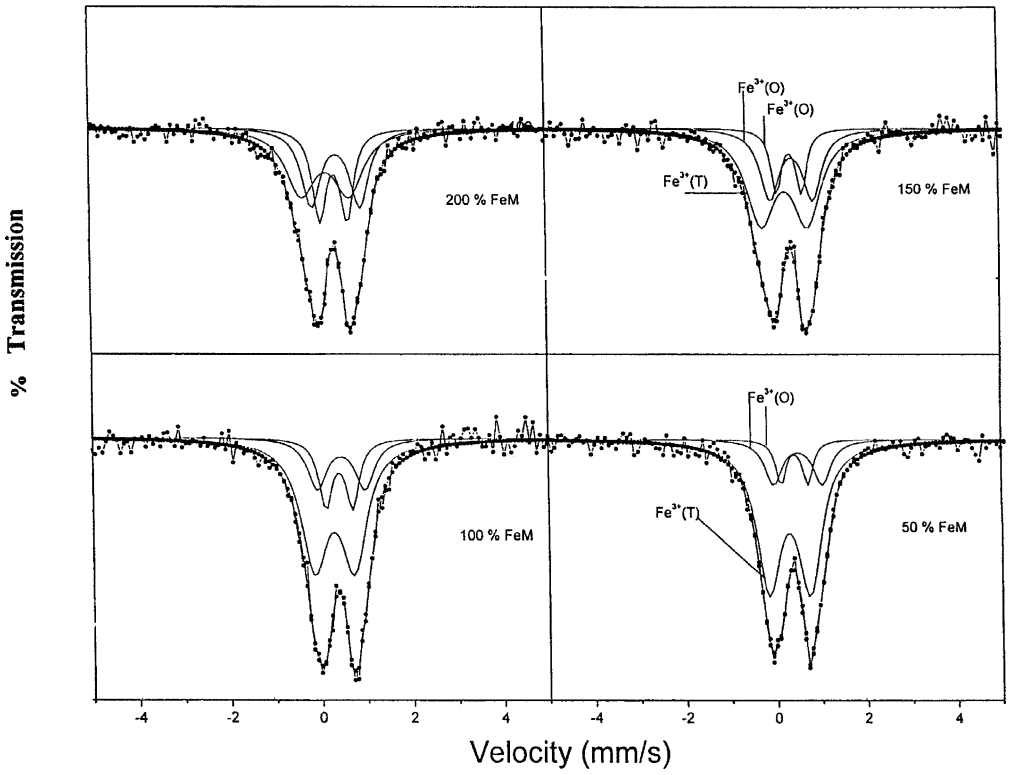

Fig. 1. Room temperature Mössbauer spectra of calcined (773 K) Fe–mordenites; prepared by liquid-state ion exchange of 50% FeM, 100% FeM, 150% FeM, and 200% FeM samples.

Table 1
Mössbauer parameters of the spectra shown in Figs. 1 and 3

	Ferric Octa [$Fe^{3+}(O)_2$]				Ferric Tetra [$Fe^{3+}(T)$]				Ferric Octa [$Fe^{3+}(O)_1$]				α-Fe_2O_3				
Sample name	IS (mm/s)	QS (mm/s)	LW (mm/s)	Area (%)	IS (mm/s)	QS (mm/s)	LW (mm/s)	Area (%)	IS (mm/s)	QS (mm/s)	LW (mm/s)	Area (%)	IS (mm/s)	QS (mm/s)	LW (mm/s)	H_{eff} (kOe)	Area (%)
50% FeM	0.40	0.59	0.27	9.8	0.27	0.91	0.64	73.6	0.48	1.08	0.46	16.6					
100% FeM	0.40	0.59	0.35	17.0	0.27	0.87	0.7	63.3	0.45	1.04	0.5	19.1					
150% FeM	0.36	0.56	0.35	17.6	0.25	1.03	0.77	56.8	0.4	0.96	0.50	26.4					
200% FeM	0.36	0.6	0.35	27	0.18	1.05	0.77	41	0.41	1.06	0.50	32					
100% FeHM					0.29	1.29	0.54	11.3					0.37	−0.211	0.35	516	76.8
					0.30	0.72	0.47	11.8									
100% $FeNH_4M$					0.29	0.93	0.76	21.3					0.37	−0.22	0.30	516	67.4
													0.27	0.28	1.48	478	11.4

Note. IS, isomer shift; QS, electric quadrupole splitting; LW, full width at half maximum; H_{eff}, mean hyperfine field.

external surfaces. These doublets could be due to Fe^{3+} in a superparamagnetic state of different particle sizes and/or due to Fe^{3+} in different distortion states, where $Fe^{3+}(O)_1$ with larger QS is in a highly unsymmetrical environment on the surface of zeolite [14]. Comparison of the samples' relative area (Table 1) shows that increasing the Fe loading causes a marked decrease in Fe^{3+} of tetrahedral symmetry, e.g., 73.6% for 50% FeM versus 41% for 200% FeM. Conceivably, the decrease in the latter was parallel to the increase in the non-framework Fe^{3+} with loadings. The decrease in $Fe^{3+}(T)$ could be due to the high calcination temperature (823 K). Similarly, Raj et al. [15] reported that the calcination of [Fe]–B zeolite at 723 K caused a partial transformation of the framework $Fe^{3+}(T)$ into extra-framework $Fe^{3+}(O)$. The crowding of Fe species with high loadings could be another plausible explanation, causing a decrease in the mean free path of Fe ions that in turn would affect the coordination numbers of $Fe^{3+}(T)$.

The MS of the samples measured at 20 K showed the disappearance of both $Fe^{3+}(O)$ phases and the appearance of a magnetic six line, which has the parameters of α-Fe_2O_3 and a broad doublet represents the framework $Fe^{3+}(T)$. These results showed that both $Fe^{3+}(O)_1$ and $Fe^{3+}(O)_2$ represent superparamagnetic α-Fe_2O_3 in different sizes. Fig. 2 shows a representative spectrum of one of the samples measured at 20 K.

The XRD results (Table 2) revealed that the Fe-containing zeolite samples exhibit the typical lines of the NaM zeo-

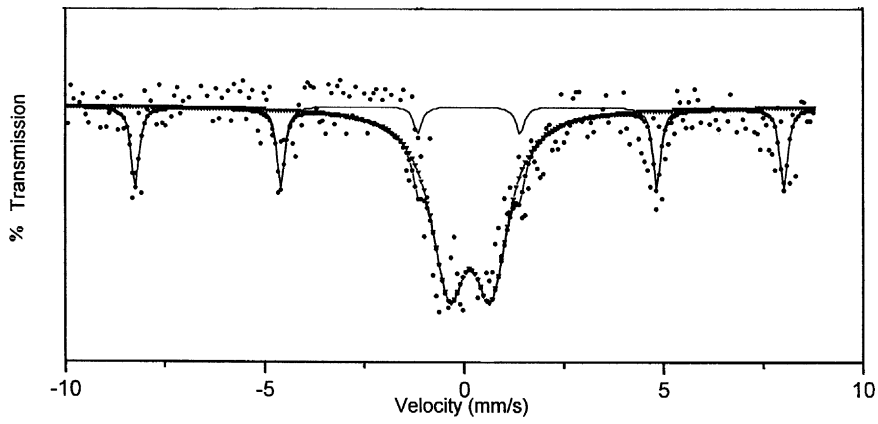

Fig. 2. A 20 K Mössbauer spectrum of the 150% FeM sample.

Table 2
X-ray data and surface characteristics of the studied samples

Sample	Preparation method	Crystallinity[a] (%)	Cell volume (Å^3)	S_{BET} (m^2/g)	S_T (m^2/g)	V_p (ml g^{-1})	r_H (Å)	BET-C constant
HM	Liquid state	100	2798	340	377	0.63	53.4	17
50% FeM	ion exchange	82	2823	485	499	0.59	30.1	30
100% FeM		77	2852	564	558	0.56	24.5	26
150% FeM		83	2902	465	477	0.60	32.9	47
200% Fe-M		80	2939	495	483	0.53	26.8	58
100% FeHM	Solid state ion	67	2806	276	269	0.45	40.5	40
100% $FeNH_4M$	exchange	67	2773	566	567	0.54	23.7	76

[a] The crystallinity was obtained from sum of the intensities of some diffraction lines. The original mordenites (NaM, HM and NH_4M) were taken as reference of 100% crystallinity. V is the unit cell volume abc, S_{BET} is the specific surface area, V_p is the total pore volume, r_H is the mean pore radius, and S_T is an additional set of specific surface areas obtained from volume–thickness curves.

lite, indicating that the structure of the zeolite remains intact after the treatment procedure. The observed decreases in the intensities of the samples (∼20%) correlate with the increasing Fe content of the samples. This decrease can be a result of the higher absorption coefficient of Fe compounds for the X-ray radiation and of the lower zeolite content in the samples. The absence of any line characteristic of Fe species suggested that either Fe substituted Al and/or occluded as fine oxides inside mordenite channels. This suggests that the loaded Fe is finely dispersed in mordenite. On the other hand, the external surface area of mordenite is small, 5 m^2/g [16]. This implies that most Fe in mordenite is present inside channels. The latter hypothesis was emphasized through the appearance of the superparamagnetic state using Mössbauer spectroscopy giving an idea about the lower limit of particle size of the non-framework Fe species. The threshold value for the appearance of the magnetic splitting, at 20 K, in the spectrum of 150 FeM is ∼2.9 nm [17]. The unit cell volume of FeM samples (50–200%) was increased monotonically with the increase in Fe contents, indicating good incorporation of Fe in mordenite channels. The latter enhancement to the cell volume could be due to the existence of an Fe–O bond (1.84 Å) instead of either a Si–O (1.60 Å) or a Al–O [18] bond.

BET measurements of the above-mentioned four samples (Table 2) showed marked increases in their total surface areas if compared with the parent Na–mordenite, suggesting the integrity of the crystal structure and the absence of pore plugging or blocking by the non-framework species. This can be due to the adsorption of the highly dispersed ironoxide particles on the external zeolite surfaces. It has been acknowledged that the estimated amounts of Fe^{3+} in octahedral symmetry can occupy charge-compensating positions [18] or leave the framework to become non-lattice species. In the latter case, these species tend to be oxidized, migrate, and sinter to form bulk oxide [19] at high temperatures. Judging from our results, such a case was not revealed, suggesting that Fe^{3+} ions were located in charge compensating positions. Additionally, the exhibited increase in surface areas of the samples with Fe loadings suggested that the octahedral iron oxide not only was in the form of highly dispersed particles but also was not attached strongly to the framework, i.e., having their own pore structure. Concerning this point more details are elaborated under Acid Leaching.

3.2. Solid-state ion exchange

Figure 3 shows the MS of the solid-state ion exchange of $FeCl_3$ (100%) with HM and NH_4M as starting materials. For the sample derived from HM, the spectrum was fitted with one magnetic sextet as well as two overlapping para-

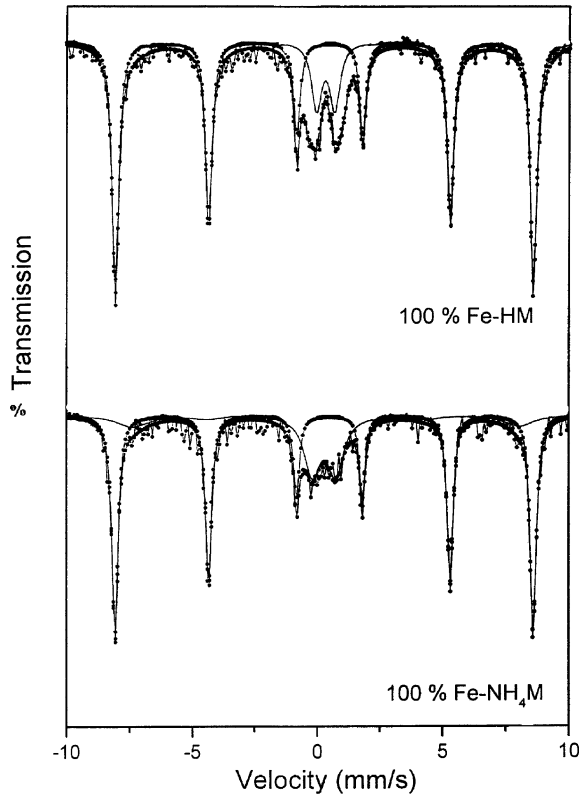

Fig. 3. Room temperature Mössbauer spectra of calcined (773 K) Fe–mordenites, prepared by solid-state ion exchange, of 100% FeHM and 100% $FeNH_4M$ samples.

magnetic doublets representing Fe^{3+} in tetrahedral sites. The Mössbauer parameters (Table 1) of the magnetic pattern revealed that about 77% of the total iron is in the form of a well-crystallized hematite phase (α-Fe_2O_3) that is localized most probably on the zeolite surface [20]. The two Fe^{3+}(T) in the framework of zeolite represent the mean extremes of a continuum of slightly different environment due to different substitutions [21].

The spectrum of the sample derived from NH_4M was fitted with two overlapping sextets representing well and poorly crystallized α-Fe_2O_3 and one central broad doublet corresponds to Fe^{3+}(T). The decrease in the hyperfine magnetic field value of the second broad α-Fe_2O_3 phase from 516 to 478 kOe as well as the marked shift in the QS value from -0.22 to 0.28 mm/s indicated that the second phase may principally be attributed to the decreased particle size [21].

The XRD measurements of the samples, derived from HM or NH_4M (Fig. 4), showed new diffraction lines at $2\theta = 33.13$, 49.85, and 54.11, which were ascribed to the most intensive lines of the hematite phase [22]. In comparison the 100% Fe sample that resulted from the liquid-state ion exchange was also included in the figure. A marked decrease in line intensities of former samples was exhibited (Table 2), indicating a marked loss in the mordenite crystal structure. This indeed indicates that α-Fe_2O_3 is formed in the mordenite channels.

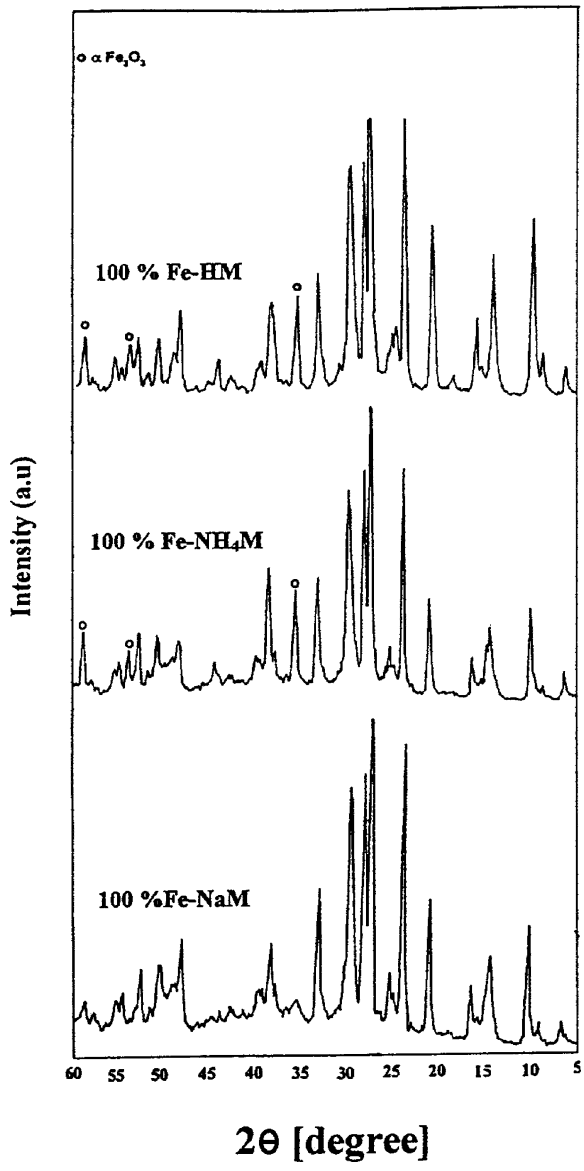

Fig. 4. Comparison of XRD patterns of 100% FeNaM, 100% FeM, and 100% $FeNH_4M$ samples.

On the other hand, the BET surface area of the sample derived from NH_4M showed a value (566 m^2/g) higher than that derived from HM (276 m^2/g), suggesting a partial plugging or blocking of the pores of the latter sample. This sample even showed surface area lower than that of the parent sample H–mordenite (340 m^2/g). In view of the Mössbauer data of the sample derived from NH_4M, the increase in the surface area may be due to exhibiting ultrafine and fine particles of α-Fe_2O_3. More information about the particles' size for this sample can be deduced if we take into account the theoretical spectra calculated by Huffman et al. [21] for α-Fe_2O_3, having different particle sizes, on the basis of the model suggested by Wickman [23] for relaxation effects in particles spin system. Accordingly, the distribution of the magnetic hyperfine field is related to and resulted from particle size distributions. Nevertheless, by comparing our field

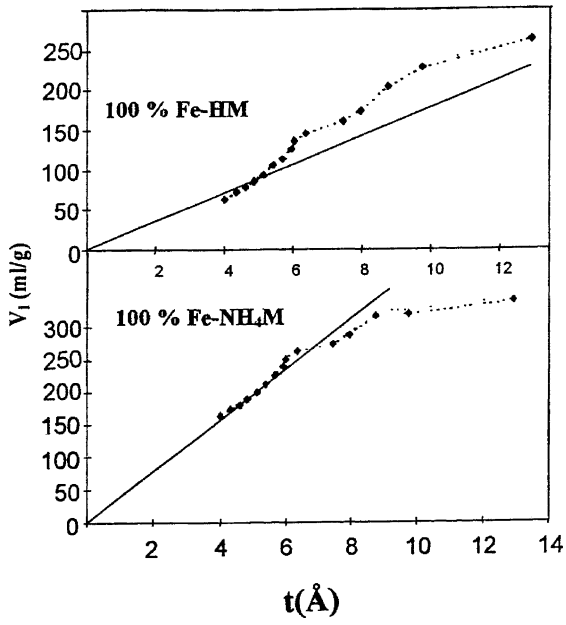

Fig. 5. V_1–t plots of 100% FeM and 100% $FeNH_4M$ samples.

values and line broadening of the Mössbauer spectrum of NH_4M with those of Huffman et al. [21], it can be seen that such subspectra in our sample correspond to definite particle sizes, i.e., two different forms of α-Fe_2O_3 due to different particle sizes. On the other hand, the Mössbauer parameters obtained for the HM sample indicate the presence of one magnetic phase of α-Fe_2O_3. I suppose the presence of such a distribution of particle sizes on the external surface of zeolite is responsible for enhancing the S_{BET} for the sample derived from NH_4M over that of HM. It is expected that the particles of α-Fe_2O_3 in the NH_4M will be found in deeper surfaces of zeolites than those in the case of HM. This can be facilitated by ammonia departure in the former [13]. Thus, it is expected that the presence of α-Fe_2O_3 near the external surface of zeolite in HM could be responsible for decreasing the S_{BET} of this sample (pore blocking). This is ascertained from the decreased pore volume of this sample when compared with all samples (Table 2). Moreover, this sample was of different reddish color suggesting the presence of α-Fe_2O_3 near the zeolite surface.

More emphasize on the pores type can be imposed from V_1–t plot (Fig. 5). The V_1–t plot obtained for the sample derived from NH_4M showed a small upward deviation noted in the t range 5.8–6.6 Å followed by a downward deviation that extended from 7 to 13 Å. This indicates the existence of both wide pores and narrow pores, respectively; however, the tendency for the latter was greatly achieved. The existence of pore narrowing (micropores) is usually correlated with an increase in the BET surface area. In contrast, the plot of the HM sample possessed a texture dominated by wide pores. This clarified the marked decrease in this sample surface area that was paralleled by a decrease in total pore volume V_p as well as by an increase in pore radius. This indicates that the pore system is not as deep as it is wide. On the other hand, the NH_4M sample exposed a texture dominated by pores narrower than those of the texture of the HM sample. During treatment the Fe species find their way to the wide pores leaving behind the narrow ones that are responsible for enhancing the area of the sample.

3.3. Acid leaching

The locations of extra-framework Fe^{3+} cations either near the surface or occluded inside zeolite channels were difficult to determine at this stage using MS. However, in order to obtain clear-cut information concerning the lat-

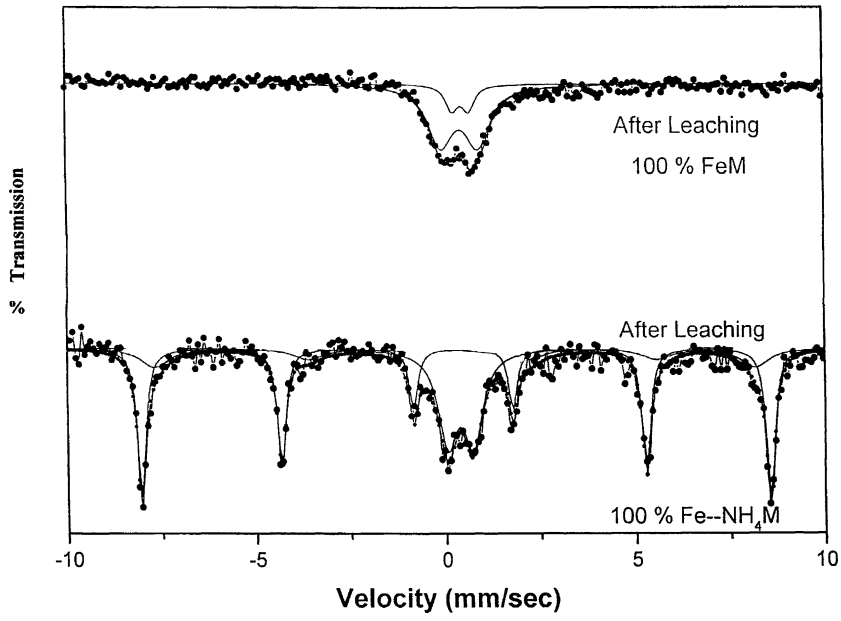

Fig. 6. Mössbauer spectra of 100% FeM and 100% $FeNH_4M$ samples after acid leaching (0.1 M HCl, 336 K).

ter issue, additional MS measurements were performed on 100% FeM and 100% $FeNH_4M$ samples, that underwent acid leaching (HCl, 0.1 M, 3 h) at 333 K. More information about the consequences of the dealumination process can be found elsewhere [24]. Prior to the measurements, the samples were washed with distilled water and finally calcined at 773 K. The acid treatment resulted in the disappearance of the most highly distorted extra-framework Fe^{3+} in the former sample (Fig. 6), which was characterized by IS = 0.45 and QS = 1.04 mm/s (Table 1, Fig. 1). This result indicates that the latter species $[Fe^{3+}(O)_1]$ was present on the external surface of the mordenite zeolite. Thus, extra-framework Fe^{3+} cations of IS = 0.40 and QS = 0.59 mm/s (Table 1) were located inside the mordenite channels.

The Mössbauer spectrum of the 100% $FeNH_4M$ sample revealed a slight reduction of the hematite phase (α-Fe_2O_3) when compared with the corresponding analog (Fig. 3) before treatment. This indicates that the majority of the hematite phase was highly dispersed on the surface of zeolite or deep inside channels.

4. Conclusions

1. The Mössbauer spectra of isomorphously substituted Fe–mordenites, which were prepared by liquid-state ion exchange, have proven the existence of framework Fe^{3+} in tetrahedral sites together with another two sites assigned to octahedral Fe^{3+} (non-framework). The latter species were located either outside or inside channels as highly dispersed particles; with diameters in the nano range, as has been evidenced by evolution of the superparamagnetic α-Fe_2O_3 at 20 K. In conformity, XRD data showed the absence of any line characteristic of Fe species.

2. The MS of the solid-state ion exchange of $FeCl_3$ with either NH_4M or HM revealed appreciable amounts of the α-Fe_2O_3 phase; however, their presence in a more dispersed form was estimated in the sample derived from NH_4M. Acid leaching gives an idea about the locations of different extra-framework Fe^{3+} cations.

References

[1] J.N. Armor, Catal. Today 26 (1995) 99.
[2] A.P. Walker, Catal. Today 26 (1995) 107.
[3] B. Coq, D. Tachon, F. Figueras, G. Mabilon, M. Pringent, Appl. Catal. B 6 (1995) 271.
[4] X. Feng, W.K. Hall, Catal. Lett. 41 (1996) 45.
[5] X. Feng, W.K. Hall, J. Catal. 166 (1997) 368.
[6] W.J. Mortier, J. Phys. Chem. 81 (1977) 1334.
[7] M.P. Attfield, S.J. Weigel, A.K. Cheetham, J. Catal. 170 (1997) 227.
[8] W.N. Delgass, R.R. Garten, M.J. Boudart, J. Phys. Chem. 73 (1969) 2970.
[9] H.-Y. Chen, E.-M. El-Malki, X. Wang, R.A. Van Santen, W.M.H. Sachtler, J. Mol. Catal. A: Chem. 162 (2000) 159.
[10] Y. Li, J.N. Armor, Appl. Catal. B 2 (1992) 239.
[11] W.K. Hall, X. Feng, J. Dumesic, R. Watwe, Catal. Lett. 52 (1999) 13.
[12] J. Bassett, R.C. Denney, G.H. Jeffery, J. Mendham, Vogel's Textbook of Quantitative Inorganic Analysis, XVIII, 1978, p. 741.
[13] M. Rauscher, K. Kesore, R. Monnig, W. Schwieger, A. TiBler, T. Turek, Appl. Catal. A 184 (1999) 249.
[14] V. Schunemann, H. Trevino, G.D. Lei, D.C. Tomczak, W.M.H. Sachtler, K. Fogash, J.A. Dumesic, J. Catal. 153 (1995) 144.
[15] A. Raj, S. Sivasanker, K. Lazar, J. Catal. 147 (1994) 207.
[16] M. El Moselhy, Master thesis, Al-Azhar University, 2001.
[17] H. Ziethen, A.X. Trautwein, Stud. Surf. Sci. Catal. 46 (1989) 789.
[18] P.A. Jacobs, in: B.C. Gates, L. Guczi, H. Knözinger (Eds.), Metal Clusters in Cataysis, Elsevier, Amsterdam, 1986.
[19] Y.-F. Chang, J.G. McCarty, Catal. Lett. 34 (1995) 163.
[20] C.D. Mariadassou, J.L. Dormann, O. Gorochov, D. Svoronos, Hyp. Inter. 28 (1986) 915.
[21] G.P. Huffman, B. Ganguly, J. Zhao, K.R.P. Rao, N. Shah, Z. Feng, F.E. Huggins, M.M. Taghiei, F. Lu, I. Wender, V.R. Pradhan, J.W. Tierney, M.S. Seehra, M.M. Ibrahim, J. Shabtai, E.M. Eyring, Energy Fuels 7 (1993) 285.
[22] M.M. Mohamed, B.A. Abu-Zeid, Thermochim. Acta 359 (2000) 109.
[23] H. Wicknan, in: I.J. Gruverman (Ed.), Mössbauer Effect Methodology, Vol. 2, Plenum, New York, 1966.
[24] M.M. Mohamed, T.M. Salama, J. Colloid Interface Sci. 249 (2002) 104.